This effect has been observed in bismuth by Mavroides *et al.*[12] However, the theory given here is not applicable to semimetals in the present form.

[12] J. G. Mavroides, B. Lax, K. J. Button, and Y. Shapira, Phys. Rev. Letters **9**, 451 (1962).

ACKNOWLEDGMENTS

The author wishes to thank Dr. G. A. Alers for communicating his results prior to publication. He is also indebted to Dr. M. J. Harrison, Dr. J. J. Quinn, and Dr. A. W. Overhauser for stimulating discussions.

PHYSICAL REVIEW VOLUME 130, NUMBER 5 1 JUNE 1963

Spin Wave Spectra of Magnetite

M. Lawrence Glasser and Frederick J. Milford
Battelle Memorial Institute, Columbus, Ohio
(Received 18 January 1963)

Expressions for spin wave energies in normal and inverse spinel have been obtained which are exact to all orders in the spin wave momentum. These dispersion curves have been compared with existing experimental data on magnetite and good agreement found if the principal exchange interaction is taken to be 2.4×10^{-3} eV. The surprisingly small range of validity of the usual k^2 approximation is pointed out and possible effects of the deviation from k^2 behavior on the magnetic part of the heat capacity are discussed. The small (like-like) exchange interactions have been included (also to all orders in the spin-wave momentum) with the most important result that agreement with the experimental dispersion curves is improved.

INTRODUCTION

MAGNETITE (Fe_3O_4) is the simplest of the so-called ferrites,[1] compounds of the form $X^{2+}(Y^{3+})_2O_4$ crystallizing in the spinel structure, (space-group $Fd3m$-O_h^7). This structure is basically cubic having in a unit cell sixteen octahedral (B) sites and eight tetrahedral (A) sites. At normal temperatures magnetite has the inverse spinel structure in which the A sites are occupied by ferric ions and the remaining ferric and ferous ions are distributed over the B sites. As the temperature is lowered below 120°K many magnetic and thermal properties undergo a sudden change. There is also a sharp drop in the electrical conductivity. This transformation was ascribed by Vervey[2] to an ordering of the ferric and ferrous ions on the B sites into alternate planes perpendicular to the C axis producing net orthorhombic symmetry. This proposal has been confirmed by neutron diffraction measurements[3] and recently by Mössbauer absorption measurements.[4] A sketch of the unit cell below the transition temperature is shown in Fig. 1.

There have been a number of calculations of the spin wave spectra in the normal and inverse spinel structure.[5–8] Most results indicate a quadratic acoustic branch. A linear behavior was found by Vonsovskii and and Seidov, but this work has been criticized by Kaplan and Kowalewski. (The latter also points out an error in Kaplan's calculation.) Apparently the only calculation for the ordered inverse spinel structure has been made by Kouvel.[9]

The ordered structure may be considered to consist of six interpenetrating face-centered cubic lattices, two consisting of A sites and four of B sites. Thus, the spin wave spectrum will have six branches. Kouvel assumed that the z axis was the single anisotropy direction and that at 0°K the A spins were down and the B spins up. Assuming only nearest-neighbor AA, BB, and AB exchange integrals he set up the (sixth degree) secular equation for the frequencies and succeeded in finding the

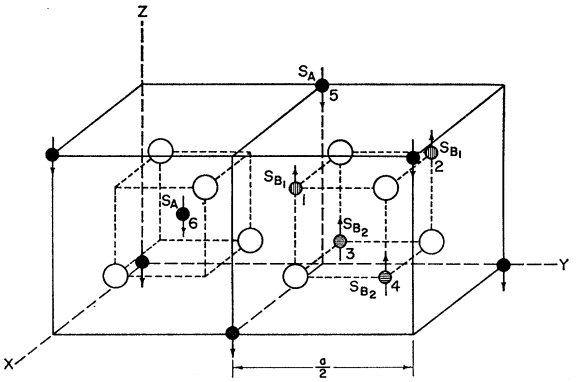

FIG. 1. One quarter of the unit cell for ordered inverse spinel. One cation site of each variety is labeled. The open circles represent oxygen sites.

[1] J. Smith and H. P. J. Wijn, *Ferrites* (John Wiley & Sons, Inc., New York, 1959).
[2] E. J. W. Verney and E. L. Heilmann, J. Chem. Phys. **15**, 174 (1947).
[3] W. C. Hamilton, Phys. Rev. **110**, 1050 (1958).
[4] R. Bauminger, S. G. Cohen, A. Marinn, and E. Segal, Phys. Rev. **122**, 1447 (1961).
[5] H. Kaplan, Phys. Rev. **86**, 121 (1952).
[6] S. V. Vonsovski, Y. M. Seidov, Izv. Akad. Nauk. SSSR **18**, 319 (1954) (translation available through Columbia Technical translations).
[7] T. A. Kaplan, Phys. Rev. **109**, 782 (1958).
[8] L. Kowalewski, Acta. Phys. Polon. **20**, 675 (1961).
[9] J. S. Kouvel, Technical Report 210, Cruft Laboratory, Harvard, 1955 (unpublished).

infinite-wavelength (ferrimagnetic resonance) modes. By making a long-wavelength expansion, he obtained the quadratic behavior of the acoustic branch.

To investigate a proposal of Unruh and Milford,[10] that deviation from the quadratic dispersion law may seriously affect the temperature dependence of the low-temperature specific heat and magnetization, we have attempted to simplify Kouvel's[11] calculation enough to obtain a more detailed description of the acoustic branch of the spin wave spectrum. In the case of vanishing exchange interactions between ions on the same type sites exact (to all orders in k^2) expressions for the spin wave energies for all directions of the wave vector have been found for wave vectors in the k_x, k_y plane for ordered inverse spinel and for more general wave vectors in normal spinel. These results have been used to estimate the accuracy of Kouvel's k^2 approximation, to construct constant energy surfaces in k space and for comparison with the neutron inelastic scattering data of Watanabe and Brockhouse.[12]

FORMULATION OF THE SPIN WAVE PROBLEM

The basic approach to this problem was worked out several years ago by Kouvel,[13] but since his work has not been published we shall outline it briefly. The spin Hamiltonian may be written

$$\begin{aligned}\mathcal{H}=&2J_{AB}\sum_{\langle ij\rangle}\mathbf{S}_i^A\cdot\mathbf{S}_j^B\\&+2J_{AA}\sum_{\langle ij\rangle}\mathbf{S}_i^A\cdot\mathbf{S}_j^A+2J_{BB}\sum_{\langle ij\rangle}\mathbf{S}_i^B\cdot\mathbf{S}_j^B\\&-\mathbf{H}\cdot\sum_i g_A\mu\mathbf{S}_i^A-\mathbf{H}\cdot\sum_i g_B\mu\mathbf{S}_j^B.\end{aligned}\tag{1}$$

According to Néel[14] the quantities J_{AB}, J_{AA}, J_{BB} (the negatives of the corresponding exchange integrals) are positive. We assume only nearest-neighbor exchange interactions and ignore anisotropy. The magnetic field H will be taken along the z axis.

The equations of motion for the spin vectors belonging to the lth A site and mth B site are

$$\begin{aligned}\hbar\mathbf{S}_1^A=i[\mathcal{H},S_1^A]=\mathbf{S}_1^A&\\\times\{-2J_{AB}\sum_i\mathbf{S}_i^B-2J_{AA}\sum_j\mathbf{S}_j^A+g_A\mu\mathbf{H}\}&\\\hbar\dot{\mathbf{S}}_m^B=\mathbf{S}_m^B\times\{-2J_{AB}\sum_i\mathbf{S}_i^A-2J_{BB}\sum_j\mathbf{S}_j^B+g_B\mu\mathbf{H}\}.&\end{aligned}\tag{2}$$

The spinel structure consists of six interpenetrating face centered cubic lattices: two consisting of A sites and four of B sites.[15] The twelve spin sums (over nearest neighbors) which are, therefore, necessary in (2) may easily be evaluated from the coordinates listed in the Appendix. For generality, we assume that there are three types of spins: A spins which occupy the A sites and B_1 and B_2 spins each of which occupy half of the B sites. To fix ideas we shall consider the ordered inverse spinel, (the structure of magnetite below 120°K) in which layers of B sites normal to the z axis are occupied alternately by B_1 and B_2 spins.

We express the spin vectors in rectangular coordinates as

$$\begin{aligned}\mathbf{S}^A&=S_x^A\hat{a}_x+S_y^A\hat{a}_y-S_z^A\hat{a}_z,\\\mathbf{S}^{Bi}&=S_x^{Bi}\hat{a}_x+S_y^{Bi}\hat{a}_y+S_z^{Bi}\hat{a}_z.\end{aligned}\tag{3}$$

In developing the equations of motion we make the spin wave approximation of considering the z components to be invariant in space and time and keeping only linear terms in the transverse components. Finally, we look for normal modes of the form:

$$\sigma_+(\mathbf{r},t)\equiv S_x+iS_y=\sigma\exp(i\mathbf{k}\cdot\mathbf{r}-i\omega t).\tag{4}$$

This leads, in the usual way, to the secular equation

$$\begin{vmatrix}U_1 & a_1 & a_2 & a_3 & b_1 & b_1^*\\ a_1 & U_1 & a_4 & a_5 & b_2 & b_2^*\\ a_2 & a_4 & U_2 & a_6 & b_3 & b_3^*\\ a_3 & a_5 & a_6 & U_2 & b_4 & b_4^*\\ b_1^* & b_2^* & b_3^* & b_4^* & U_3 & c^*\\ b_1 & b_2 & b_3 & b_4 & c & U_3\end{vmatrix}=0.\tag{5}$$

The off-diagonal quantities are sums over nearest-neighbor spins and are given by

$$\begin{aligned}a_1&=-4J_{BB}\cos[(a/4)(k_x-k_y)],&a_4&=-4J_{BB}\cos[(a/4)(k_y+k_z)],\\a_2&=-4J_{BB}\cos[(a/4)(k_x+k_z)],&a_5&=-4J_{BB}\cos[(a/4)(k_x-k_z)],\\a_3&=-4J_{BB}\cos[(a/4)(k_y-k_z)],&a_6&=-4J_{BB}\cos[(a/4)(k_x+k_y)],\\b_1&=-2J_{AB}([\bar{3}\bar{1}1]+[131]+[1\bar{1}\bar{3}]),&b_3&=-2J_{AB}([3\bar{1}\bar{1}]+[\bar{1}3\bar{1}]+[\bar{1}\bar{1}3)],\\b_2&=-2J_{AB}([311]+[\bar{1}\bar{3}1]+[\bar{1}1\bar{3}]),&b_4&=-2J_{AB}([\bar{3}1\bar{1}]+[1\bar{3}\bar{1}]+[113]),\\&&c&=-2J_{AA}([\bar{2}\bar{2}\bar{2}]+[22\bar{2}]+[\bar{2}22]+[2\bar{2}2]),\end{aligned}\tag{6}$$

[10] H. Unruh, Jr., and F. J. Milford, Phys. Rev. **123**, 1619 (1961).
[11] J. S. Kouvel, Phys. Rev. **102**, 1489 (1956).
[12] H. Watanabe and B. N. Brockhouse, Phys. Letters **1**, 189 (1962).
[13] J. S. Kouvel, Tech. Report 210, Cruft Laboratory, Harvard, 1955 (unpublished).
[14] L. Néel, Ann. Phys. **3**, 137 (1948).
[15] E. W. Gorter, Philips Research **9**, 295 (1954).

where, for example,

$$[m\bar{n}l]=\exp[i(a/8)(mk_x-nk_y+lk_z)] \tag{7}$$

and a is the lattice parameter. Also,

$$\begin{aligned} U_1S_{B_1}=W_1&=[\hbar\omega-12J_{AB}S_A+4J_{BB}(S_{B_1}+2S_{B_2})-g_B\mu H],\\ U_2S_{B_2}=W_2&=[\hbar\omega-12J_{AB}S_A+4J_{BB}(S_{B_2}+2S_{B_1})-g_B\mu H],\\ -U_3S_A=-W_3&=[\hbar\omega+12J_{AB}(S_{B_1}+S_{B_2})-8J_{AA}S_A-g_A\mu H]. \end{aligned} \tag{8}$$

The approximations that have been made in obtaining (5) are

(1) The linear spin wave approximation in which second-order terms in S_x and S_y are neglected in the equations of motion.

(2) Only nearest-neighbor interactions are included.

(3) The approximations inherent in the Hamiltonian (1).

It is perhaps worth noting that an alternative approach is to transform the Hamiltonian to harmonic oscillator form and identify the products of coefficients of squares of canonically conjugate variables as eigenfrequencies. This procedure produces results which are identical with the equation of motion approach wherever they can be compared. Using the transformed Hamiltonian to obtain equations of motion may, however, introduce spurious factors of $S/[S(S+1)]^{1/2}$ due to the replacement of S_{op}^2 by $S(S+1)$ unless great care is exercised. This problem is well known and much discussed[16–18] in connection with the ground-state energy.

SPECIAL CASE $J_{AA}=J_{BB}=0$

It is generally felt that in magnetic materials with the spinel structure J_{AA} and J_{BB} are much smaller than J_{AB}. Since quantitative experimental information on the relative sizes of the exchange constants is extremely difficult to obtain it is common to approximate this situation by $J_{AA}=J_{BB}=0$. In this case all of the a_i's and c are zero and the secular equation reduces to[19]

$$\begin{aligned} W_1^4W_3^2-2W_1^3W_3[S_{B_2}S_A(b_3^*b_3+b_4^*b_4)+S_{B_1}S_A(b_1^*b_1+b_2^*b_2)]-W_1^2S_A^2\{S_{B_2}^2(b_3^*b_4-b_4^*b_3)^2+S_{B_1}^2(b_1^*b_2-b_1b_2^*)^2\\ +S_{B_1}S_{B}[(b_1^*b_4-b_4^*b_1)^2+(b_1^*b_3-b_3^*b_1)^2+(b_2^*b_4-b_4^*b_2)^2+(b_2^*b_3-b_3^*b_2)^2]\}=0. \end{aligned} \tag{9}$$

This equation may be solved readily with no further approximation to give

$$\begin{aligned} \hbar\omega_1&=\left|-6J_{AB}(S_{B_1}+S_{B_2}-S_A)+\left\{36J_{AB}^2(S_{B_1}+S_{B_2}-S_A)^2+144J_{AB}^2S_A(S_{B_1}+S_{B_2})+\frac{B}{2}+\tfrac{1}{2}(B^2-4C)^{1/2}\right\}^{1/2}\right|,\\ \hbar\omega_2&=\left|-6J_{AB}(S_{B_1}+S_{B_2}-S_A)-\left\{36J_{AB}^2(S_{B_1}+S_{B_2}-S_A)^2+144J_{AB}^2S_A(S_{B_1}+S_{B_2})+\frac{B}{2}+\tfrac{1}{2}(B^2-4C)^{1/2}\right\}^{1/2}\right|,\\ \hbar\omega_3&=\left|-6J_{AB}(S_{B_1}+S_{B_2}-S_A)+\left\{36J_{AB}^2(S_{B_1}+S_{B_2}-S_A)^2+144J_{AB}^2S_A(S_{B_1}+S_{B_2})+\frac{B}{2}-\tfrac{1}{2}(B^2-4C)^{1/2}\right\}^{1/2}\right|,\\ \hbar\omega_4&=\left|-6J_{AB}(S_{B_1}+S_{B_2}-S_A)-\left\{36J_{AB}^2(S_{B_1}+S_{B_2}-S_A)^2+144J_{AB}^2S_A(S_{B_1}+S_{B_2})+\frac{B}{2}-\tfrac{1}{2}(B^2-4C)^{1/2}\right\}^{1/2}\right|, \end{aligned} \tag{10}$$

$$\hbar\omega_5=\hbar\omega_6=12JS_A,$$

where

$$\begin{aligned} B&=-2[S_{B_2}S_A(b_3^*b_3+b_4^*b_4)+S_{B_1}S_A(b_1^*b_1+b_2^*b_2)],\\ C&=-S_A^2\{S_{B_2}^2(b_3^*n_4-b_4^*b_3)^2+S_{B_1}^2(b_1^*b_2-b_2^*b_1)^2\\ &\qquad S_{B_1}S_{B_2}[(b_1^*b_4-b_4^*b_1)^2+(b_1^*b_3-b_3^*b_1)^2+(b_2^*b_4-b_4^*b_2)^2+(b_2^*b_3-b_3^*b_2)^2]\}. \end{aligned} \tag{11}$$

A similar set of solutions has been found by Kaplan[7] for normal spinel. The energies are easily evaluated for interesting values of the spins and arbitrary momenta. The important thing, of course, is that no restriction to small momenta is involved.

One of the most interesting structures to which (10) can be applied is magnetite which is an ordered inverse spinel below 119°K and an inverse spinel with a random distribution of equal numbers of ferrous and ferric ions between the two kinds of B sites above this

[16] R. S. Smith and M. J. Klein, Phys. Rev. **80**, 111 (1950).
[17] P. W. Anderson, Phys. Rev. **83**, 1260 (1951).
[18] R. Kubo, Phys. Rev. **87**, 568 (1952).
[19] F. J. Milford and M. L. Glasser, Phys. Letters **2**, 248 (1962).

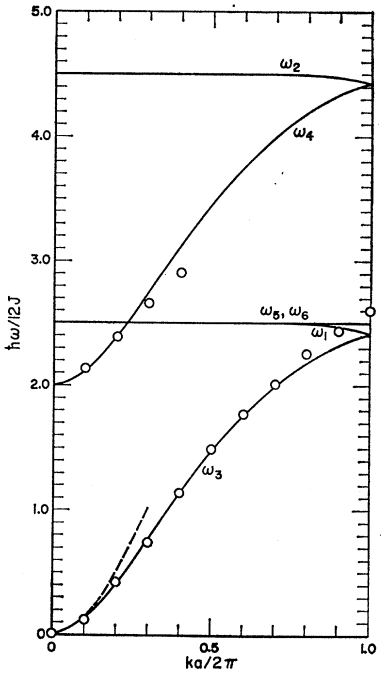

FIG. 2. Dispersion curves for ordered inverse spinel with $J_{AA}=J_{BB}=0$. Circles are the Watanabe and Brockhouse experimental data reduced assuming $J_{AB}=2.4\times10^{-3}$ eV. Broken curve is Kouvel's k^2 approximation.

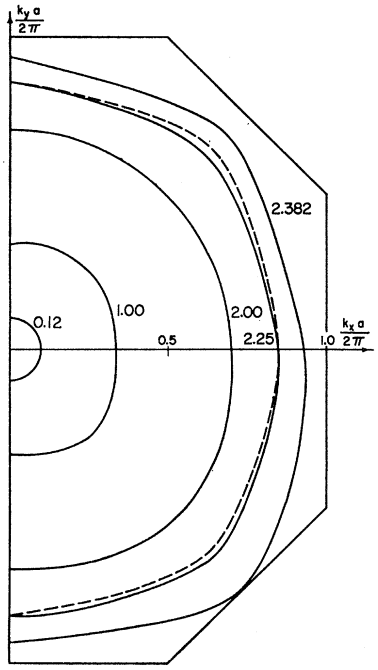

FIG. 4. Constant energy contours in k_x, k_y plane. Energies are labeled in units of $12J_{AB}$. Broken curve is for normal spinel and energy $\hbar\omega/12J_{AB}=2.25$ and illustrates fourfold symmetry in that case.

temperature. For the ordered configuration, (10) and (11) apply with $S_A=S_{B_1}=2.5$, $S_{B_2}=2$. Using these values of the spins one obtains the dispersion curves shown in Fig. 2 for the spin wave momentum k in the z direction. The lowest mode for several other directions all of which are in the k_y-k_y plane are shown in Fig. 3.

It may be noted again[12,19] that the dispersion curve in the z direction agrees quite well with the neutron scattering work of Watanabe and Brockhouse as may be seen from the experimental points which are plotted assuming $J_{AB}=2.4\times10^{-3}$ eV. As Kaplan[20,21] has shown and as is further discussed later in this work, including the J_{BB} interaction improves the agreement. Even without this refinement, however, the agreement is sufficiently good to encourage further study of the model.

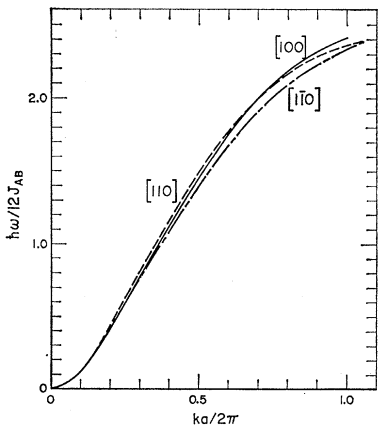

FIG. 3. Dispersion curves for three directions in the k_x, k_y plane.

The dispersion curves for momenta perpendicular to the z direction also provide interesting information. Kouvel[13] has shown that to order k^2 the constant energy surfaces are ellipsoids with principal axes in the [001], [110] and [1$\bar{1}$0] directions in k space but has not estimated the range of k for which the approximation is valid. The range of validity of the k^2 approximation is surprisingly small and may be conveniently estimated by taking k in the x direction. In this case to order k^2

$$\hbar\omega_3=\frac{11}{16}\frac{J_{AB}S_A(S_{B_1}+S_{B_2})}{S_{B_1}+S_{B_2}-S_A}k^2a^2. \tag{12}$$

This is a special case of Kouvel's more general k^2 approximation and is also easily obtained by approximating (10) to order k^2. If $ka/2\pi=0.1$ the k^2 approximation gives $\hbar\omega_3/12J_{AB}=0.127$ while the exact value is 0.119, an error of 6%. The error increases rapidly with increasing k and is about 25% at $ka/2\pi=0.2$. The k^2 approximation is shown as a broken line in Fig. 2. The deviation of the exact result from the k^2 approximation is such that the constant energy surfaces do not have ellipsoidal shapes for $ka/2\pi\gtrsim0.1$. The point is made clear for rather large values of $ka/2\pi$ by Fig. 4 which shows actual cross sections of constant energy surfaces. It should be noted that the total deviation from sphericity is not great for $ka/2\pi=0.8$. In fact, the 3% spread in k reported by Brockhouse and Watanabe[21] for five directions with $\hbar\omega=0.0493$ eV is essentially sufficient to

[20] T. A. Kaplan, Lincoln Laboratory, Solid State Research Report, 1962 (unpublished).
[21] B. N. Brockhouse and H. Watanabe, Atomic Energy of Canada Report AECL 1575, and IAEA Symposium on Inelastic Scattering of Neutrons (to be published).

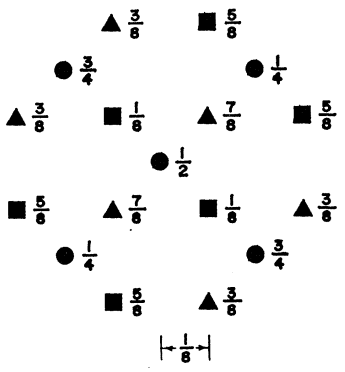

FIG. 5. Nearest neighbors of an A ion. Solid circles are A ions, squares B_1 ions, and triangles B_2 ions. Numbers next to symbols are z coordinates in units of the lattice parameter. Scale in projection plane is indicated also in units of the lattice parameter.

accommodate the differences among the dispersion curves of Fig. 3. Experiments for larger energy momentum transfers should show deviations from sphericity at least at temperatures below the ordering temperature.

In view of the unusual shapes of the constant energy surfaces it is perhaps worth commenting on the symmetry of magnetite. The symmetry of ordinary spinel is that of the space-group $O_h^7(Fd3m)$. Inverse spinel may be reasonably expected to have the same symmetry in some average sense as long as it is not ordered. Ordering, however, seems to reduce the symmetry, perhaps to T_d, but no detailed crystallographic investigation of this point is known to us. (Lyons *et al.*[22] have discussed the question in a certain framework but this may not be adequate for determining the symmetry of the energy surfaces.) No serious conflicts arise except possibly as to whether the k_z axis is one of twofold or fourfold symmetry. It is clearly twofold for ordered inverse spinel, fourfold for normal and probably effectively fourfold for disordered inverse spinel as may be seen from Fig. 5. In this figure the 16 nearest neighbors of a tetrahedral site are shown. The fact that a rotation through $\pi/2$ does not produce the same structure is evident as is the fact that the z axis is not a fourfold screw axis. If the distinction between B_1 and B_2 spins disappears the z axis becomes a fourfold screw axis and this in turn leads to

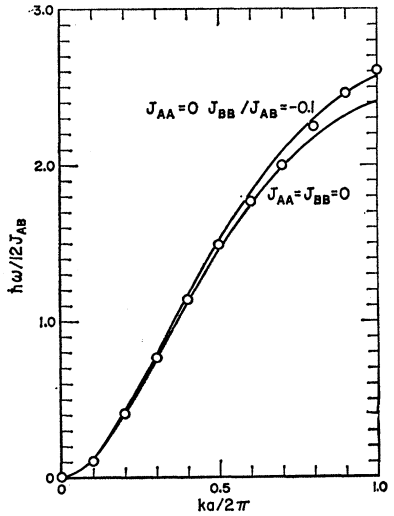

FIG. 6. Acoustic spin wave dispersion curve for $J_{BB}=-0.1J_{AB}$ together with Watanabe and Brockhouse experimental points and acoustic mode from Fig. 2. $S_{B_1}=S_{B_2}=2.25$.

fourfold symmetry in the constant energy surfaces. One section of a surface with fourfold symmetry and $\hbar\omega/12J_{AB}=2.25$ and $S_A=2.5$, $S_{B_1}=S_{B_2}=2.25$ is shown in Fig. 4.

It should also be noted that the difference between the results for $S_{B_1}=S_{B_2}=2.25$ and those for $S_{B_1}=2.5$, $S_{B_2}=2.0$ is quite small in the principle crystallographic directions. This is particularly evident from a comparison of Figs. 2 and 6.

EXACT SOLUTION FOR J_{AB}, $J_{BB}\neq 0$

Another approach to the solution of the secular equation is required if the exchange interactions between like spins are not negligible. For $k_z=0$ the secular equation may be factored into two cubics. To do this we note that by adding successive rows and columns in pairs the secular equation may be put in the form

$$\begin{vmatrix} 2(U_1+a_1) & \alpha & \beta_{12} & U_1+a_1 & a_3+a_5 & b_1^*+b_2^* \\ \alpha & 2(U_2+a_6) & \beta_{34} & a_4+a_5 & U_2+a_6 & b_3^*+b_4^* \\ \beta_{12} & \beta_{34} & 2U_3+c+c^* & b_2+b_2^* & b_4+b_4^* & U_3+c^* \\ 2(U_1+a_1) & 2(a_4+a_5) & 2(b_2+b_2^*) & 2U_1 & 2a_5 & 2b_2^* \\ 2(a_3+a_5) & 2(U_2+a_6) & 2(b_4+b_4^*) & 2a_5 & 2U_2 & 2b_4^* \\ 2(b_1+b_2) & 2(b_3+b_4) & 2U_3+2c & 2b_2 & 2b_4 & 2U_3 \end{vmatrix} = \begin{vmatrix} \Delta_{11} & \Delta_{12} \\ \Delta_{21} & \Delta_{22} \end{vmatrix}, \tag{13}$$

where $\beta_{ij}=b_i+b_j+b_i^*+b_j^*$, $\alpha=a_2+a_3+a_4+a_5$, and the Δ's are 3×3 matrices.

When $k_z=0$, $a_2=a_5$, $a_3=a_4$, $b_3=b_4^*$, $b_1=b_2^*$, and $c=c^*$. In this case (13) clearly has the form

$$\begin{vmatrix} \Delta_{11} & \Delta_{12} \\ \Delta_{11} & \Delta_{22} \end{vmatrix} = \begin{vmatrix} \Delta_{11} & \Delta_{12} \\ 0 & \Delta_{22}' \end{vmatrix}, \tag{14}$$

and consequently factors into $|\Delta_{11}|\cdot|\Delta_{22}'|$. Thus, the roots in this case are given by the solutions of the two cubic equations

$$\begin{vmatrix} U_1+a_1 & a_2+a_3 & b_1+b_2 \\ a_2+a_3 & U_2+a_6 & b_3+b_4 \\ b_1+b_2 & b_3+b_4 & U_3+c \end{vmatrix} = 0 \tag{15}$$

and

$$\begin{vmatrix} U_1-a_1 & a_2-a_3 & b_1-b_2 \\ a_2-a_3 & U_2-a_6 & b_3-b_4 \\ b_2-b_1 & b_4-b_3 & U_3-c \end{vmatrix} = 0. \tag{16}$$

[22] D. H. Lyons, T. A. Kaplan, K. Dwight, and N. Menyuk, Phys. Rev. **126**, 540 (1962).

These equations may be solved analytically without making any further approximations to yield the dispersion curves in the central plane of the Brillouin zone. For example, when $k=0$:

$$\begin{aligned} &a_1=a_2=a_3=a_4=a_5=a_6=-4J_{BB},\\ &b_1=b_2=b_3=b_4=-6J_{AB},\\ &c=c^*=-8J_{AA},\ \beta_{ij}=2b_1,\ g_B\mu H=Z_B,\ g_B\mu H=Z_A. \end{aligned} \tag{17}$$

Making these substitutions in (16) we find $(U_1+4J_{BB})\times(U_2+4J_{BB})(U_3+8J_{AA})=0$, so that

$$\begin{aligned} \hbar\omega_2&=|12J_{AB}(S_{B_1}+S_{B_2})-16J_{AA}S_A-Z_A|,\\ \hbar\omega_1&=\hbar\omega_0=|12J_{AB}S_A-8J_{BB}(S_{B_1}+S_{B_2})+Z_B|. \end{aligned} \tag{18}$$

If the second two rows of (15) are added to the first row and the first column subtracted from the second column (15) takes on the form

$$\begin{vmatrix} \hbar\omega-Z_B & 0 & \hbar\omega-Z_A \\ 2a_1S_{B_2} & \hbar\omega+2b_1S_A-Z_B+2a_1(S_{B_1}+S_{B_2}) & 2b_1S_{B_2} \\ -2b_1S_A & 0 & \hbar\omega-2b_1(S_{B_1}+S_{B_2})-Z_A \end{vmatrix}=0. \tag{19}$$

This is immediately solved to give

$$\begin{aligned} \hbar\omega_5&=|12J_{AB}S_A-8J_{BB}(S_{B_1}+S_{B_2})+Z_B|,\\ \hbar\omega_4&=\tfrac{1}{2}|Z_A+Z_B+2b_1(S_{B_1}+S_{B_2}-S_A)+\{[Z_A-Z_B+2b_1(S_{B_1}+S_{B_2}-S_A)]^2+8b_1S_A(Z_A-Z_B)\}^{1/2}|,\\ \hbar\omega_3&=\tfrac{1}{2}|Z_A+Z_B+2b_1(S_{B_1}+S_{B_2}-S_A)-\{[Z_A-Z_B+2b_1(S_{B_1}+S_{B_2}-S_A)]^2+8b_1S_A(Z_A-Z_B)\}^{1/2}|. \end{aligned} \tag{20}$$

(These values are in disagreement with those of Kouvel[13] which may easily be seen to be in error by taking all of the exchange constants equal to zero.) If the Zeeman terms are disregarded ω_3 vanishes, and therefore, represents the acoustic mode. In the case that $S_{B_1}+S_{B_2}$ is less than $2S_A$, (15) will give the lowest three branches of the dispersion relation (if in addition J_{AA}, J_{BB} are much smaller than J_{AB}, which is usually the case).

One of the most useful applications of this procedure is the investigation of the influence of finite exchange interactions between like spins on the acoustic branch of the dispersion curve. To illustrate the effect we have calculated the acoustic branch for k in the x direction and $J_{BB}=0$ and $J_{BB}=-J_{AB}/10$. For this direction of $\mathbf{k}$ and $\mathbf{H}=0$ the acoustic mode energies are given by

$$\frac{\hbar\omega}{12J_{AB}}=\left|\frac{S_A-2S_B}{2}-\frac{1}{3}\left(\frac{J_{BB}}{J_{AB}}S_B-\frac{J_{AA}}{J_{AB}}S_A\right)\gamma+\left\{\left[\frac{S_A+2S_B}{2}-\frac{1}{3}\left(\frac{J_{BB}}{J_{AB}}S_B+\frac{J_{AA}}{J_{AB}}S_A\right)\gamma\right]^2-\frac{2}{9}S_AS_B\beta^2\right\}^{1/2}\right|, \tag{21}$$

where $\gamma=(1-\cos ka/4)$, $\beta=2\cos(ka/8)+\cos(3ka/8)$ and for simplicity $S_{B_1}=S_{B_2}=S_B>S_A/2$. The numerical results for $S_A=2.50$, $S_B=2.25$ in the two cases noted above are shown in Fig. 6. These results agree exactly with those obtained by Kaplan[20,21] and for $J_{BB}/J_{AB}<0$ clearly tend to improve the agreement with the Watanabe and Brockhouse[12,21] measurements. It should be noted that if $S_{B_1}=S_{B_2}$ the factorization of the sixth-order secular equation into two cubics can also be accomplished for k in the z direction. Furthermore, the roots are the same as those found for k in x direction as indeed must be the case from symmetry considerations. Thus, the comparison with the Watanabe and Brockhouse experimental data is appropriate. A small J_{AA} does not affect the dispersion curves appreciably because of the sign alternation between the two places where it appears in (21).

DISCUSSION

As a result of this careful study of the dispersion curves in spinel structures a number of interesting points have emerged. In accord with the original motivation for this work major deviations of the acoustic mode dispersion curve from a k^2 behavior are found. The actual curves are in good agreement with the experimental results of Watanabe and Brockhouse[12,21] and may bear importantly on the heat capacity question. The original difficulty was that heat capacity measurements on magnetite[11] when interpreted on the basis of spin wave theory gave exchange constants which were smaller by a factor of about four than those obtained from the Curie temperature on the basis of molecular field theory. Similar discrepancies in other ferrites including the system $Ni_{1-x}Fe_{2+x}O_4$ were observed by Pollack and Atkins.[23] The latter results together with those of Kouvel[11] for magnetite lie on a smooth curve when plotted versus composition but this is not a stringent test of Kouvel's measurements. The situation is now somewhat worse since spin wave theory has been shown to account in detail for the directly observed dispersion curves using an exchange interaction much larger than that required by the heat capacity data. This situation is summarized in Table I. It has been suggested that

TABLE I. Values of the exchange constant.

Source	Exchange constant (eV)
Curie temperature	1.6×10^{-3}
Heat capacity	0.44×10^{-3}
Dispersion curve	2.4×10^{-3}

[23] S. R. Pollack and K. R. Atkins, Phys. Rev. 125, 1248 (1962).

improvements in the interpretation of T_c might give better agreement[23] with the heat capacity result but this would leave a serious discrepancy when compared with the dispersion curve result. It seems more likely that the heat capacity result is in error. This could be due to errors in the measurement but this seems unlikely especially in light of the work of Pollack and Atkins. A second possibility is that the ordering which takes place in magnetite below 119°K makes the comparison of heat capacity results with those obtained from Curie temperature measurements and neutron inelastic scattering inappropriate. Such a difference can only be due to a major change in the exchange interaction caused by the crystallographic distortion below 119°K since it has been shown in this work that the ordering has little effect on functional form of the dispersion curves which play the central role in the heat capacity calculation. This point could be decided by means of low temperature neutron inelastic scattering experiments. Another possibility which we believe has considerable promise is that the laborious calculations of the heat capacity from the dispersion curves have not been done sufficiently accurately. This point has been discussed in an earlier paper[10] but for simpler cubic lattices. It is now being investigated for the spinel structure on the basis of the dispersion curves presented here.

The lack of fourfold symmetry in the constant spin wave energy surfaces in ordered magnitite has also been noted. It would be interesting, although perhaps very difficult, to verify the twofold symmetry experimentally by means of inelastic scattering experiments at temperatures below 119°K. Such low-temperature experiments would also, as noted earlier, establish an exchange constant of unequivocable appropriatness for comparison with the low-temperature heat capacity result.

Finally, the effect of small exchange interactions between like ions has been computed and shown to improve the agreement with the inelastic scattering data. The inclusion of $J_{BB}=-0.1J_{AB}$ seems to be all that is required. This is not expected to modify the heat capacity results in a significant way. Values of J_{AA} smaller than $0.1J_{AB}$ do not produce significant changes in the dispersion curves.

ACKNOWLEDGMENTS

We are indebted to a number of people for helpful discussions of various points. Professor J. R. Reitz, Professor C. S. Smith, Professor M. J. Klein, and Professor S. A. Freidburg have made particularly useful comments. Professor B. N. Brockhouse has made available preprints of his recent work and informed us of Dr. T. A. Kaplan's contemporaneous work on the subject. Battelle Memorial Institute has supplied generous financial support and encouragement.

APPENDIX

Lists of nearest neighbors for computing spin sums. The coordinates are given in units of $a/8$; the bar denotes a negative value. Where only one set is listed, the second consists of the negatives of the first set.

Nearest neighbors to an A site at (0,0,0)

B_1	$(\bar{1},\bar{3},\bar{1})$	$(1,3,\bar{1})$	
	$(\bar{3},\bar{1},\bar{1})$	$(\bar{1},1,3)$	
	$(3,1,\bar{1})$	$(1,\bar{1},3)$	
A sites	$(\bar{2},\bar{2},\bar{2})$	$(2,2,\bar{2})$	
	$(2,\bar{2},2)$	$(\bar{2},2,2)$	
B_2 sites	$(1,1,\bar{3})$	$(1,\bar{3},1)$	
	$(\bar{1},\bar{1},\bar{3})$	$(\bar{1},3,1)$	
	$(3,\bar{1},1)$	$(\bar{3},1,1)$	

Nearest neighbors to a B_1 site at (0,0,0)

A sites	Set I	$(\bar{3},\bar{1},1)$	$(1,\bar{1},\bar{3})$	$(\bar{1},\bar{3},\bar{1})$
		$(1,3,1)$	$(3,1,\bar{1})$	$(\bar{1},1,3)$
	Set II	$(3,1,1)$	$(\bar{1},1,\bar{3})$	$(1,3,\bar{1})$
		$(\bar{1},\bar{3},1)$	$(\bar{3},\bar{1},\bar{1})$	$(1,\bar{1},3)$
B_1 sites		$(2,\bar{2},0)$		
		$(\bar{2},2,0)$		
B_2 sites	Set I	$(\bar{2},0,\bar{2})$	$(0,\bar{2},2)$	
		$(2,0,2)$	$(0,\bar{2},2)$	
	Set II	$(2,0,\bar{2})$	$(0,\bar{2},\bar{2})$	
		$(\bar{2},0,2)$	$(0,2,2)$	

Nearest neighbors to a B_2 site at (0,0,0)

A sites	Set I	$(3,\bar{1},\bar{1})$	$(\bar{1},\bar{1},3)$	$(1,\bar{3},1)$
		$(\bar{1},3,\bar{1})$	$(\bar{3},1,1)$	$(1,1,\bar{3})$
	Set II	$(\bar{3},1,\bar{1})$	$(1,1,3)$	$(\bar{1},3,1)$
		$(1,\bar{3},\bar{1})$	$(3,\bar{1},1)$	$(\bar{1},\bar{1},\bar{3})$
B sites	Set I	$(2,0,2)$	$(0,2,2)$	
		$(\bar{2},0,\bar{2})$	$(0,\bar{2},\bar{2})$	
	Set II	$(\bar{2},0,2)$	$(0,\bar{2},\bar{2})$	
		$(2,0,\bar{2})$	$(0,2,\bar{2})$	
B_2 sites		$(\bar{2},\bar{2},0)$		
		$(2,2,0)$		